UNIVERSITY of
BRADFORD

Library

The University of Bradford Institutional Repository

http://bradscholars.brad.ac.uk

This work is made available online in accordance with publisher policies. Please refer to the repository record for this item and our Policy Document available from the repository home page for further information.

To see the final version of this work please visit the publisher's website. Access to the published online version may require a subscription.

Effect of the addition of different waste carbonaceous materials on coal gasification in CO_2 atmosphere

Ashak M. Parvez [a], Iqbal M. Mujtaba [b], Chengheng Pang [a], Tao Wu [a,*]

[a] Department of Chemical and Environmental Engineering, The University of Nottingham Ningbo China, Ningbo 315100, China

[b] Chemical Engineering Division, School of Engineering , University of Bradford, Bradford BD7 1DP, UK

Corresponding author: Tao.Wu@nottingham.edu.cn

Abstract

In order to assess the utilisation of waste carbonaceous materials and the feasibility of using CO_2 as a gasifying agent, the gasification characteristics of coal, a suite of waste carbonaceous materials, and their blends were investigated by using a thermogravimetric analyser (TGA). The results showed that the CO_2 gasification process of polystyrene completed at 470 °C which was lower than other carbonaceous materials. This behaviour was attributed due to the high content of volatile coupled with its unique thermal degradation properties. It is found that the initial decomposition temperature decreased with the increasing amount of waste carbonaceous materials in the blends. Overall, CO_2 co-gasification process was enhanced as a direct consequence of interactions whose intensity and temperature of occurrence were influenced by the chemical and compositional properties of carbonaceous materials. The strongest interactions were noticed in coal/polystyrene blend at the devolatilisation stage as indicated by its highest value of Root Mean Square Interaction Index (RMSII), caused by highly reactive characteristic of polystyrene. On the other hand, coal/oat straw blend revealed the highest interactions at char gasification stage. The catalytic effect of alkali metals content in oat straw, particularly CaO and K_2O, was believed to be the reasons

23 for these strong interactions. Furthermore, co-pyrolysis was compared with CO_2 gasification

24 through RMSII value, while the effect of CO_2 as a gasifying agent on interactions during co-

25 gasification was also evaluated. It is clear from this study that CO_2 gasification of coal can be

26 enhanced significantly via the addition of polystyrene and oat straw.

27 **Keywords**: CO_2 gasification; Carbonaceous materials; Interactions; Catalytic effect

1 Introduction

29 In order to minimise CO_2 emissions, different waste carbonaceous materials are used as

30 energy source because of their carbon neutral nature. In recent years, co-utilisation of waste

31 carbonaceous materials has become increasingly popular to replace a portion of coal in

32 existing coal-fired boilers for power generation [1, 2].

33 Over the years, many techniques have been developed to utilise coal with biomass and other

34 carbonaceous materials. Co-gasification is one of the promising methods because it has the

35 potential to improve the gas yield and corresponding heating value of the product when low

36 quality coal is gasified [3, 4]. Moreover, improved overall carbon conversion and cold gas

37 efficiency can also be achieved by increasing the proportion of biomass in the feed.

38 For gasification process, CO_2 is a potential gasification medium [5-7]. It is less corrosive than

39 steam and can be used to adjust syngas composition for different applications [8]. In the past

40 decades, a lot of research has been carried out on biomass gasification using CO_2 as a

41   gasifying agent [5, 7, 9-12]. These researches were mainly focused on the kinetics [5, 9, 11,

42   12], gasification reactivity [7, 10, 13, 14] and gasification characteristics [14-16] in general.

43   In spite of huge potential of CO_2 in coal and biomass gasification, limited effort have been

44   made to understand gasification behaviours, particularly on interactions during co-gasification.

45   Apart from these, limited study has been conducted understanding how to enhance co-

46   gasification via choosing suitable waste carbonaceous materials for the co-gasification of

47   certain coal. In addition, information on waste carbonaceous materials such as non-metallic

48   part of printed circuit boards, tyre scraps and polystyrene are very limited compared with the

49   conventional fuel and biomass. Moreover, not much work has been performed to understand

50   the effects of CO_2 on the gasification process of these carbonaceous materials. Thus, there are

51   still needs to achieve in depth understanding of gasification characteristics of coal, waste

52   carbonaceous materials and their blends.

53   In this paper, gasification characteristics of coal, a suite of waste carbonaceous materials and

54   their blends were investigated in a TGA using CO_2 as the only gasifying agent. In addition,

55   the influence of mass fractions of carbonaceous materials on gasification characteristics of the

56   blends was analysed. The interactions during co-gasification were also studied and the reasons

57   for these interactions were explored.

2 Experimental

2.1 Samples preparation

In this study, an Australian bituminous coal was selected as the coal sample. Oat straw (OS), Non-metallic part of printed circuit boards (NMPCBs), tyre scraps (tyre) and polystyrene (PS) were chosen as the waste carbonaceous materials samples. All samples were air-dried at ambient temperature prior to further processing. Size reduction was carried out by using an industrial hammer crusher (CSF570, Fengli Pulverization Ltd., China) and ball mill (SM2000, MM400, Retsch, Germany), respectively. All samples were ground to a size smaller than 106 microns (Endecott 106 microns aperture sieve) following the standard milling procedure (CEN/TS 15443:2006). Before characterization and testing, all samples were treated following international accepted standard procedure to ensure representativeness of the samples [17].The blend samples were prepared from these materials by mixing manually at (coal to waste carbonaceous material) mass ratios of 90:10 and 70:30 (with a maximum deviation of ± 0.1 mg), which is denoted as high and low bending ratios, respectively. These ratios are representative of typical co-gasification parameters, corresponding to 5%-35% on thermal basis.

2.2 Sample characterisation

Proximate analysis of the samples was conducted based on the standard practice for Proximate Analysis using a TGA following procedures described elsewhere [18] . All the

77   experiments were repeated three times and average value was used for the study. Carbon (C),

78   hydrogen (H), nitrogen (N) and sulphur (S) contents were determined using a CHNS/O

79   Element Analyser (PE2400, PerkinElmer, USA) following the standard testing procedure

80   described in the manual. The standard sample was firstly applied to calibrate the Elemental

81   Analyser. Approximately 1.5 mg of dried fine powder was used for each test, which was

82   repeated at least three times. Oxygen content was calculated by difference on dry and ash free

83   basis. The tests were carried out in helium carrier gas with an accuracy of ≤0.3% and a

84   precision of ≤0.2%. Calorific value of all the samples was determined using a calorimeter

85   (IKA C 200, Germany), which was calibrated prior to testing using benzoic acid to achieve a

86   relative standard deviation less than 0.2%. As for ash composition, each sample was analysed

87   twice using an X-Ray Diffraction (XRD) (Bruker D8 Advance, Germany) to minimize

88   experimental error to be within ±1.5%.

89   ## 2.3 CO_2 gasification

90   CO_2 gasification of the coal, waste carbonaceous materials and their blends was carried out

91   using a STA 449/F3 Jupiter thermal analyser (NETZSCH Geraetebau GmbH, Germany) with

92   a weighing precision of ± 0.01% and TGA resolution of 0.1 μg. In each test, the sample was

93   heated to 50 °C in N_2 (30 ml/min) from room temperature and kept isothermal for 10 min. It

94   was then heated from 50 to 1200 °C at a constant heating rate of 20 K/min in the presence of

95   pure CO_2 (40 ml/min). Prior to each test, the sample was further manually grounded to

96   smaller than 90 microns to minimize diffusion effects. About 5 mg of sample (accuracy up to

97   0.01 mg via PerkinElmer AD 6 autobalance) was loaded into a ceramic crucible for each test.

98   This slow heating rate and small amount of sample used would minimise mass transfer effects

99   and eliminate the heat transfer limitations in the CO_2 gasification process. Each test was

100   repeated three times to minimize the experimental error.

2.4   Interactions indexes

102   Thermal characteristics of coal, waste carbonaceous materials and their blends in CO_2

103   atmosphere were extracted from the TG/DTG profiles. The theoretical TG/DTG curves of the

104   blends were calculated by Eq. (1) based on the mass loss rates of each individual sample

105   assuming additive property applies. The deviation between experimental and calculated

106   curves was used to show the degree of interactions between samples [19, 20]:

107
$$\frac{dm}{dt} = x_{SP1}\left(\frac{dm}{dt}\right)_{SP1} + x_{SP2}\left(\frac{dm}{dt}\right)_{SP2} \tag{1}$$

108   where $\left(\frac{dm}{dt}\right)_{SP1}$ and $\left(\frac{dm}{dt}\right)_{SP2}$ are the mass loss rates (%/min) of individual samples while

109   x_{SP1} and x_{SP2} are the corresponding mass fractions in the blends, respectively. The Root

110   Mean Square Interactions Index (RMSII) was applied to quantify the interactions between

111   components in the blend which compares the deviation of calculated value with experimental

112   value. Normally, a higher value of RMSII indicates a larger interaction taking place in the

113   process. The RMSII can be calculated using the Eq. (2) [21].

$$114 \quad RMSII = \sqrt{\dfrac{\sum\limits_{i=1}^{N} \left(\dfrac{(dm/dt)_{EXP}^{i} - (dm/dt)_{CAL}^{i}}{(dm/dt)_{CAL}^{i}} \right)^{2}}{N}} \qquad\qquad (2)$$

115   where $(dm/dt)_{EXP}$ and $(dm/dt)_{CAL}$ denote experimental and calculated mass loss rates values,

116   respectively. N represents the number of points undertaken.

117   ## 3   Results and discussion

118   ### 3.1   Properties of the samples

119   Table 1 shows proximate, ultimate and ash analysis results of the samples studied in present

120   work. For the proximate analysis, the relative standard deviation was ± 3 wt%, while for

121   ultimate analysis, it was ± 2 wt%. As can be seen, volatile content and oxygen content varied

122   significantly. Among all the tested samples, NMPCBs had the highest percentage of ash,

123   which is mainly due to the presence of glass fiber. Hence, it would have some influence on

124   gasification process. It is clear that tyre showed very similar properties in term of proximate

125   and ultimate analysis data as coal. Its heating value is also very close to that of coal. Therefore,

126   it is expected that the co-gasification of tyre with coal would have very little influence on the

127   overall gasification process. On the other hand, negligible amount of ash was detected in

128   polystyrene, which was completely decomposed, resulting in no fixed carbon formed after

129   pyrolysis. Besides, polystyrene contained no sulphur and low percentage of nitrogen

130   compared with the other samples.

131 Higher heating value (HHV) of individual samples were also included in Table 1 with relative

132 standard deviation controlled within ±4.5%. It is clear that polystyrene (41.7 MJ/kg, daf)

133 exhibited the highest heating value, greater than that of coal (35.5 MJ/kg, daf). Meanwhile,

134 the heating values of tyre (33.2 MJ/kg, daf) and NMPCBs (31.5 MJ/kg, daf) were all slightly

135 lower than coal. Hence, blend with polystyrene, tyre or NMPCBs might not have a negative

136 impact on co-gasification process. In contrast, oat straw (19.5 MJ/kg, daf) had the lowest

137 heating value, which subsequently would result in a lower gasification temperature. As

138 moderate low gasification temperature is one of the desired properties of the fuel, thus, it

139 would enhance gasification performance in co-gasification process.

140 **Table 1: Proximate, ultimate analyses and calorific values of the samples.**

	AC	OS	NMPCBs	Tyre	PS
HHV (MJ/kg dry ash free)	35.5	19.5	31.5	33.2	41.7
Proximate analysis (wt %)					
Moisture	0.7	4.2	0.8	0.4	0.9
Volatile matter	34.6	70.7	25.1	62.9	99.1
Fixed carbon	48.2	18.2	6.9	19.6	-
Ash	16.5	6.9	67.2	17.1	-
Ultimate analysis [a,b] (wt %)					
C	81.3	37.4	39.8	80.9	92.1
H	4.9	5.3	3.6	6.4	7.7
O^C	9.7	47.9	55.7	10.7	-
N	1.9	2.3	0.6	0.5	0.2
S	2.2	0.2	0.3	1.5	-
Ash composition (wt %, standard deviation ±5%)					

|					
SiO$_2$	42.6	43.3	29.7	38.5	-
SO$_3$	1.4	3.4	-	6.2	-
CaO	4.2	10.6	5.3	3.5	-
Na$_2$O	2.3	2.6	1.4	2.7	-
Fe$_2$O$_3$	7.4	0.9	4.6	45.1	-
MgO	2.2	4.2	-	0.7	-
Al$_2$O$_3$	39.1	2.2	5.3	2.4	-
K$_2$O	0.8	32.8	-	0.9	-
CuO	-	-	38.4	-	-
ZnO	-	-	5.7	-	-
Ni$_2$O$_3$	-	-	9.6	-	-

[a]Dry basis. [b]Ash free basis. [c]By difference.

3.2 Thermal behaviours of the individual samples

Fig. 1 shows the TGA and DTG curves of coal and different waste carbonaceous materials under CO_2 gasification. In this study, the instrument was calibrated to ensure that the precision of ≤0.2% in TGA analysis was achieved. In Fig. 1, it is apparent that the gasification processes involved a multi-stage thermal degradation where the number of stages and the unique features of individual stage varied. The main mass losses in coal gasification took place at 400-570 °C and 935-1190 °C, respectively (Fig. 1a). The first mass loss was due to the release of volatiles while char gasification and thermal decomposition of minerals contributed to the second mass loss. As expected in CO_2 gasification, the heterogeneous reaction between coal char and CO_2 was much slower compared with combustion process. This is because CO_2 is a weak oxidizing agent and the CO_2 gasification via Boudouard reaction (C (S) + CO_2 → 2CO) is slow [22, 23]. Normally, at atmospheric pressure, the

9

153   Boudouard reaction is thermodynamically favourable at temperatures above 900 °C (initiated

154   at 800 °C) while the combustion of char can occur at significantly lower temperatures (below

155   630 °C). Two stages of mass losses were observed in oat straw as seen in Fig. 1b. The first

156   loss (240-375 °C) was attributed to the complete decomposition of hemi-cellulose and

157   cellulose and the partial decomposition of lignin [20, 24, 25]. The decomposition of

158   remaining lignin, char gasification and minerals decomposition contributed to the second

159   mass loss (820-950 °C). Unlike coal, CO_2 gasification of char derived from oat straw took

160   place at a lower temperature range. In general, biomass has a higher amount of volatiles

161   which generate a highly porous char compared with char derived from coal [26]. The porous

162   structure of char facilitates CO_2 diffusion, which leads to a better gasification performance.

163   The gasification of oat straw therefore completed at lower temperatures. It was reported that

164   the reactivity of biomass char is usually higher than the chars produced from coal [27, 28].

165   This implies that compared with coal char, biomass char can be gasified at much lower

166   temperature which is the case for oat straw.

167   Fig. 1c shows the main mass loss experienced by NMPCBs in the second stage which is

168   illustrated at temperature from 295 to 410 °C. In spite of NMPCBs having the lowest

169   volatiles, its maximum mass loss was occurred at low temperature region.

(a)

(b)

(c)

(d)

(e)
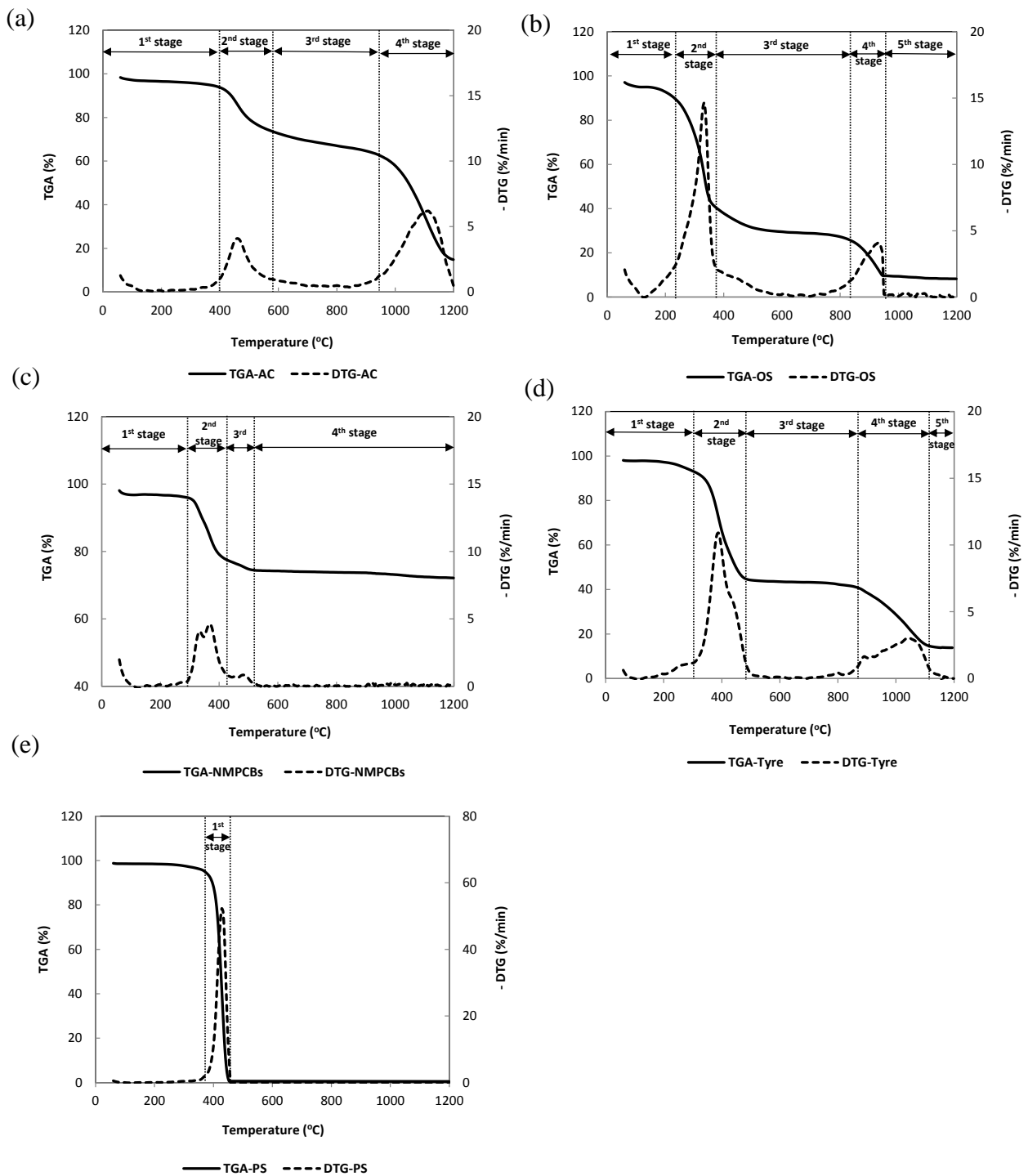
Figure 1: CO$_2$ gasification distribution of the TGA and DTG curves of (a) coal, (b) oat straw, (c) NMPCBs, (d) tyre and (e) polystyrene.

Typically, epoxy resin is the major component of the NMPCBs which is mixed with brominated compounds [29, 30]. The decomposition of epoxy resin, degradable part of NMPCBs, started at around 300 °C. Consequently, thermal decomposition of NMPCBs

11

176   consists of two stages, the decomposition of brominated compounds and decomposition of

177   non-brominated compounds. The possible reason for the existence of small peak before the

178   main peak was the partial overlapping of these two reactions [30]. As seen in Fig. 1c, a

179   smaller DTG peak which was situated between the temperatures of 465 to 510 °C, denoted the

180   second main mass loss due to the release of volatiles due to the decomposition of brominated

181   compounds in NMPCBs. It is important to notice that the value of this mass loss rate was

182   smaller (0.85 wt%/min) in comparison with mass loss rates noticed in other samples. As seen

183   in Fig. 1d, tyre also exhibited the first mass loss at low temperature region (300-490 °C)

184   similar to NMPCBs while the second mass loss happened at relatively high temperature

185   region (875-1110 °C). Generally, tyre contains small portion of additives (less than 30 wt%)

186   and the rest is rubber (natural and synthetic) [31, 32]. The first mass loss was caused by the

187   decomposition of the additives and both types of rubber which occurred at lower temperature.

188   Afterwards, the second mass loss depicted CO_2 char gasification. Higher percentage of carbon

189   in tyre might be the reason for this slow gasification reaction. On the other hand, polystyrene

190   experienced a single stage degradation at a higher temperature region (350-455 °C) compared

191   with other waste carbonaceous materials. From Fig. 1e, it can be seen that polystyrene had a

192   negligible mass loss up to 250 °C, whereas a slight mass loss was detected at temperature

193   between 250 to 350 °C. This confirmed that polystyrene was thermally stable up to 350 °C.

194   Degradation completed at 455 °C and during this stage the mass loss observed was 98.5 wt%

195   due to the thermal cracking of light organics and other carbonaceous heavy organics to low

196   molecular weight compounds. The overall mechanism is believed to be dictated by the

197   combination of end-chain initiation, depolymerisation, intramolecular hydrogen transfer, and

198   bimolecular termination processes. The changes in mass loss are caused by inter-molecular

199   transfer reactions while devolatilisation is governed by intramolecular transfer reactions.

200   Above 455 °C, no residue was observed, which confirmed the complete degradation of

201   polystyrene in CO_2 gasification. In general, gasification characteristics such as initial

202   decomposition temperature and final mass loss temperature are the crucial parameters of the

203   fuel performance. As can be seen in Fig. 1, oat straw had the lowest initial decomposition

204   temperature (281 °C). In contrast, coal and polystyrene experienced the two highest initial

205   decomposition temperatures (415 and 407 °C). However, the final maximum mass loss

206   temperatures was in the order of polystyrene (428 °C), NMPCBs (479 °C) and oat straw (931

207   °C), respectively which suggested that polystyrene and NMPCBs were more reactive

208   compared with oat straw. Moreover, the highest maximum mass loss rate (49.7 wt%/min) and

209   the lowest gasification time (18.9 min) were observed for polystyrene. Therefore, the use of

210   polystyrene as a fuel for co-gasification application would be more beneficial.

211   **3.3 Co-gasification characteristics of coal and carbonaceous materials**

212   Fig. 2 describes the co-gasification behaviours of coal and carbonaceous materials and the

213   characteristics of individual samples and blends are listed in Table 2.

(a)

(c)

(b)

(d)

214
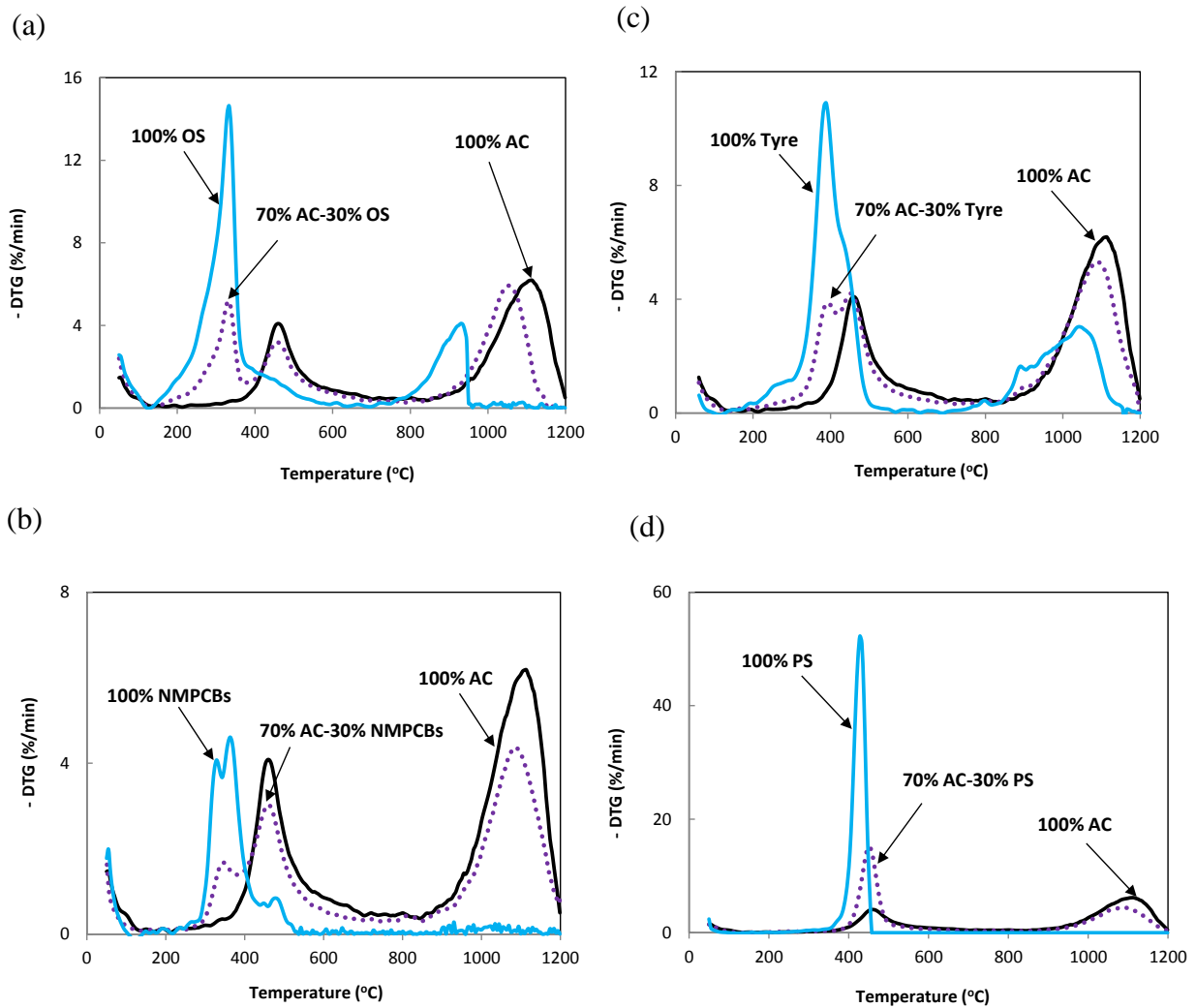
Figure 2: CO$_2$ gasification distributions of (a) coal/oat straw, (b) coal/NMPCBs, (c) coal/tyre and (d) coal/polystyrene blends (standard deviation ± 1.3%).

217   In general, curves of the blends were found in the location between those of the original

218   samples. From Fig. 2a, it is clear that coal/oat straw blends had three-stage mass loss rather

219   than the two-stage mass loss identified for the original oat straw sample. In the case of blends,

220   the first mass loss was mainly due to the volatiles release from decomposition of

221   hemicellulose and cellulose in oat straw whereas the third one was mostly caused by char

222   gasification. Commonly, the initial devolatilisation temperature of coal is approximately the

223   same as the terminal devolatilisation temperature of biomass. Therefore, the second mass loss

14

224 was attributed mainly to the devolatilisation of coal, while the gasification of chars derived

225 from both oat straw and coal collectively resulted in the third mass loss. As shown in Table 2,

226 the coal (415 °C) started to devolatilise at a higher temperature than that of the oat straw (281

227 °C). In addition, the maximum mass loss temperatures of coal and oat straw were 458/1108

228 °C and 332/931 °C, respectively. It is interesting to see that the first and the second mass loss

229 temperatures of the blends did not vary significantly. However, the change of the third mass

230 loss temperatures was noticed. This indicated that the blending of oat straw with coal did not

231 have significant influence on the devolatilisation stage but affected the char gasification

232 process. Besides, as oat straw percentage in blend increased, the reduction in the initial

233 decomposition temperature (T_i) of the blends was also observed, which contributed to a lower

234 devolatilisation temperature in co-gasification process. The experimental results also

235 demonstrated that the addition of oat straw shifted the CO_2 gasification process to a low

236 temperature region by reducing the overall maximum mass loss temperatures (T_{max}). The

237 higher volatiles content in oat straw (shown in Table 1) was the reason for these phenomena

238 as oat straw burns at a much lower temperature compared with coal. Besides, DTG value of

239 the first mass loss increased (1.9 wt%/min to 5.2 wt%/min due to increment of blending

240 proportion from 10% to 30%) due to higher volatiles content while it decreased (6 wt%/min

241 to 5.9 wt%/min) in the third mass loss due to increasing amount of the char derived from coal.

242

Table 2: CO_2 gasification characteristic parameters of blends and individual samples.

Sample	T_i	T_{max} (°C)	t_{max} (min)	DTG_{max} (%/min)
Australian coal	415	458/1108	20.5/52.8	4.1/6.1
Blend 1 (10% oat straw)	301	335/460/1091	14.2/20.5/52.2	1.9/3.9/6
Blend 2 (30% oat straw)	294	333/456/1053	14.1/20.3/50.1	5.2/3.2/5.9
Oat straw	281	332/931	14.1/44.2	14.7/4.1
Blend 1 (10% NMPCBs)	407	456/1100	20.6/53.2	3.8/5.9
Blend 2 (30% NMPCBs)	353	344/453/1082	14.7/20.5/51.7	1.7/3.0/4.3
NMPCBs	305	364/479	15.7/21.5	4.5/0.9
Blend 1 (10% tyre)	400	457/1106	20.5/52.7	4.2/5.9
Blend 2 (30% tyre)	365	395/458/1088	17.3/20.3/51.8	3.9/4.2/5.3
Tyre	357	394/1046	17.2/50.1	10.4/3
Blend 1 (10% PS)	412	456/1104	20.2/52.5	7.3/5.6
Blend 2 (30% PS)	410	453/1082	20/51.8	15.1/4.5
Polystyrene (PS)	407	428	18.9	49.7

244   T_i=Initial decomposition temperature, T_{max}= Maximum mass loss temperature, t_{max}=maximum

245   reaction time and DTG_{max}= Maximum mass loss rate.

246   Uncertainty of temperature: ±1°C. Uncertaintty of DTG_{max}: ±0.15 %/min.

247   When NMPCBs was gasified with coal at the high blending ratio, the gasification process

248   featured three main mass loss stages as seen in Fig. 2b. The first mass loss stage occurred at

249   temperature between 330 and 380 °C where the decomposition of NMPCBs took place. The

250   second DTG_{max} (400-485 °C) indicated the release of volatiles from both coal and NMPCBs

251   whereas the third DTG_{max} depicted the stage of CO_2 gasification of NMPCBs and coal

252   derived chars. In contrast, at low blending ratios, such as 10 wt% NMPCBs, only two main

253   mass loss stages were noticed at similar temperature ranges as coal in co-gasification. Here,

254   the value of first DTG_{max} (Table 2) decreased because of the lower amount of volatiles in the

255 blend contributed by NMPCBs. Meanwhile, the decrement of the second DTG_{max} was as a

256 result of the lower amount of NMPCBs char. From Table 2, it is clear that the initial

257 devolatilisation temperature and the first DTG_{max} temperature of the blend were shifted to a

258 lower temperature region as the proportion of NMPCBs increased while the final DTG_{max}

259 temperature was also shifted to a lower temperature due to the reduced amount of coal derived

260 char. Therefore, it can be concluded that the co-gasification of coal and NMPCBs completed

261 at a relatively lower temperature despite of a slight reduction of the maximum mass loss rate.

262 For coal/tyre blends as presented in Fig. 2c, two-stage mass loss was noticed at the low

263 blending ratio. The results on gasification parameters listed in Table 2 demonstrated that coal

264 had a dominant effect on the blend of 10 wt% tyre since it showed similar behaviours with the

265 characteristics of coal. It's mainly because coal and tyre have similar physical and chemical

266 properties as shown in Table 1. These properties were assumed as a result of the narrow

267 difference of initial decomposition temperatures between coal (415 °C) and tyre (357 °C), and

268 also a very small amount of tyre being blended. In contrast, the blend of 30 wt% tyre

269 experienced three-stage mass loss. From Table 2, it can be found that the first and the second

270 mass loss of the blend occurred at the same temperature as the first mass loss of original tyre

271 and coal, respectively. This means that the decomposition of tyre and coal in the blend was

272 took place sequentially rather than simultaneously. However, it can be seen from Fig. 2c that

273 gasification was shifted toward lower temperature with the increase of tyre fraction in the

274 blends. The reason behind the shifting was because of the thermal properties of tyre which

275 decomposes relatively lower temperature than coal. Besides, the third mass loss rate which

276 represented the char gasification of both coal and tyre was reduced (about 10% because of

277 increment of blending proportion from 10% to 30%) due to the low amount of char generated

278 from coal in the blend.

279 Among all the blend samples investigated in this study, coal/polystyrene blends exhibited

280 different behaviours as illustrated in Fig. 2d. As polystyrene decomposed through a single-

281 stage mass loss without any solid residue and its initial decomposition took place at a slightly

282 slower temperature than coal, a complete coincidence between whole polystyrene mass loss

283 and first mass loss of coal was observed. Hence, devolatilisation stage of the blend samples

284 was represented by a single peak in DTG profile. Compared with coal, polystyrene contained

285 approximately three times higher amount of volatiles, which resulted in the substantial

286 increment of the first mass loss rates in blends. Similar to other blends, a gradual decrement

287 of the second mass loss rate was observed when polystyrene was blended with coal. At the

288 same time, the temperature corresponding to the maximum mass loss was also reduced. This

289 was affected by the combination of the decrease in the percentage of coal and the increment

290 of volatiles from polystyrene in the blends.

3.4 Interactions between coal and carbonaceous materials

To further understand the interactions in blend, the experimental and calculated DTG curves

of the blends under CO_2 atmosphere are compared in Fig. 3. Overall, the curves illustrate that

the interactions existed as the experimental curves of blends deviated from the calculated

curves for the same blends [19, 20]. However, the deviation was not consistent at different

stages of the entire process and varied with the blending of different materials, blending ratio

and temperature range. From Fig. 3a, deviations were observed for coal/oat straw blends at

two different temperature regions. This indicated the existence of significant interactions in

the range of 950-1200 °C and weaker interactions between 390-700 °C for both high and low

blending ratios. Similarly, as seen in Fig. 3d, coal/polystyrene blends also showed significant

interactions at different temperature ranges of 400-500 °C and 1000-1200 °C. For

coal/NMPCBs blends (Fig. 3b), analogous behaviours were noticed where stronger and

weaker interactions occurred in the temperatures ranges of 1050-1200 °C and 600-900 °C,

respectively. Correspondingly, Fig. 3c depicted that in temperature range of 1160-1200 °C,

coal/tyre blends experienced noticeable interactions while insignificant interactions occurred

from 400 to 600 °C.

In order to determine the intensity of the interactions in the whole process, the root mean

square interactions index (RMSII) of the blends (as detailed in Eq. 2) were also evaluated and

listed in Table 3, which is of an accumulated uncertainty of ±0.01. Overall, the presence of

310   interactions was evident in the blends as demonstrated by RMSII value. From Table 3, it is

311   apparent that the higher the amount of carbonaceous material was added into the blend, the

312   higher the value of RMSII was observed. Moreover, regardless of blending ratio, RMSII

313   values of char gasification stage were higher than those of devolatilisation stage, except for

314   polystyrene, which ratified the strong interactions during char gasification stage. However,

315   significant interactions were noticed in devolatilisation stage for coal/polystyrene blends as

316   demonstrated by high RMSII value. At both blending ratios, the highest RMSII values in

317   devolatilisation and char gasification stages were exhibited by coal/polystyrene blends and

318   coal/oat straw blends, respectively. It is important to point out that the interactions in char

319   gasification stage of coal/NMPCBs blend at high blending ratio were considerably lower than

320   those of other ash containing blends. As seen in Table 1, NMPCBs had the highest ash

321   content (67.2 wt%) among all the carbonaceous materials studied. Thus, the high ash content

322   of NMPCBs which subsequently result in ash inhibition effect contributing to its weakest

323   interactions [33].

324   Table 4 shows the comparison of RMSII values between co-pyrolysis and CO_2 co-gasification

325   processes which were conducted under the same temperature but different atmosphere. From

326   Table 4, it is apparent that coal/oat straw blend showed higher interactions during gasification

327   process as demonstrated by its RMSII value which was over two times higher than that of

20

328 pyrolysis process. The reasons behind the aforementioned characteristics can be well

329 explained as follows.

330 It was observed that DTG curves for the devolatilisation stage in pyrolysis were similar to

331 those in CO_2 gasification so that the main DTG_{max} was almost coincided each other at the

332 same temperature. With the increase of temperature (above 900 °C), considerable additional

333 weight loss was noticed in CO_2 gasification process. This was because of the reaction of CO_2

334 with the remaining char (mostly) (Eq. 3) as CO_2 has reaction activity at high temperature

335 condition [34, 35]. Thus, it is confirmed that char gasification process played a key role for

336 these interactions.

337 $C + CO_2 \rightarrow 2CO$ (3)

338 Similarly, enhanced interactions were noticed for the blends of coal with each NMPCB and

339 tyre in CO_2 co-gasification. However, the enhancements in these blends were considerably

340 lower than that of coal/oat straw blend. This was due to the fact that char derived from

341 biomass are normally more reactive compared with those derived from other carbonaceous

342 materials such as NMPCBs. Furthermore, this phenomenon might be originated from mineral

343 content in these samples which will be discussed in the following section. Exceptionally,

344 coal/polystyrene blend had a slightly lower RMSII value in CO_2 gasification process which

345 revealed weaker interactions than in its pyrolysis process. This indicated the influence of CO_2

346 in polystyrene devolatilisation process as the contribution of $C + CO_2$ reaction is extremely

347 small since char content was literally zero. It is reported that the devolatilisation of

348 polystyrene mainly occurred because of the breaking of C-C and C-H bonds [36]. During CO_2

349 gasification, CO_2 reacts randomly with these bonds [34]. Hence, coal/polystyrene blend is

350 likely to demonstrate less interaction in this process as also presented in Table 4. Thus, it can

351 be summarised that char gasification process increased the interactions on blends of oat straw,

352 NMPCBs and tyre with coal while the devolatilisation process had a significant role on

353 coal/polystyrene blend. Nonetheless, it is interesting to note that coal/polystyrene blend

354 revealed the highest interactions in both processes as shown by its highest RMSII values

355 compared to the other blends. This was due to the high volatiles content in polystyrene sample

356 which will be detailed in section 3.5.

357 The aforementioned discussion has suggested that the mechanism of interactions between coal

358 and carbonaceous materials were highly influenced by the properties and percentage of

359 carbonaceous materials being added into the blends. Furthermore, the effect of CO_2 as

360 gasification agent on interactions was also noticed.

361 **Table 3: RMSII value of experimental and calculated DTG curves.**

Carbonaceous materials	RMSII (SD±0.01)			
	Devolatilisation		Char gasification	
	10%	30%	10%	30%
Oat straw	0.10	0.09	0.26	0.71
NMPCBs	0.13	0.25	0.20	0.24
Tyre	0.06	0.10	0.18	0.60
Polystyrene	0.32	0.92	0.13	0.17

362   **Table 4: Comparison of RMSII values between co-gasification and co-pyrolysis processes (70:30 blends).**
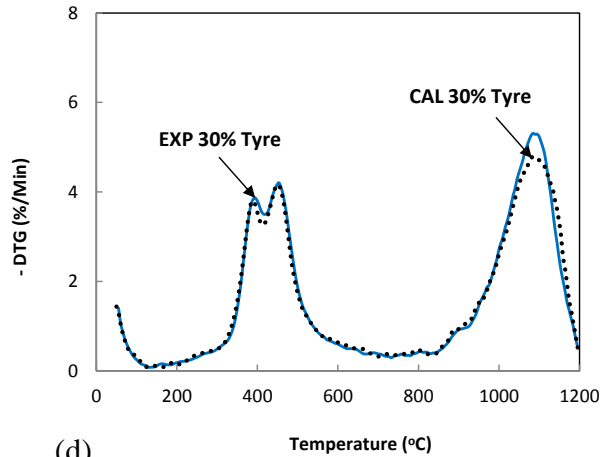
Blends	CO$_2$ co-gasification	Co-pyrolysis
AC/OS	0.43	0.20
AC/NMPCBs	0.25	0.22
AC/tyre	0.29	0.25
AC/PS	0.56	0.60

363

364   (a)   (c)
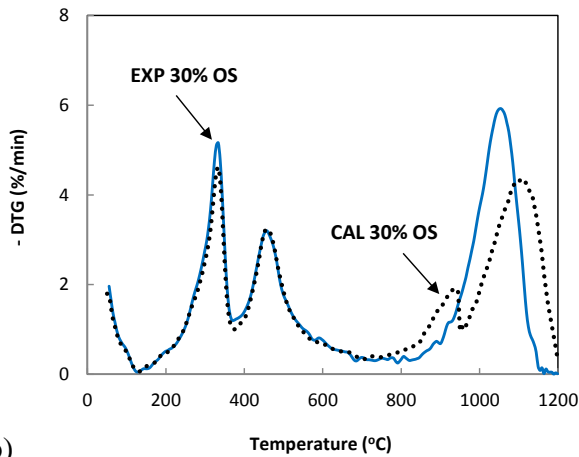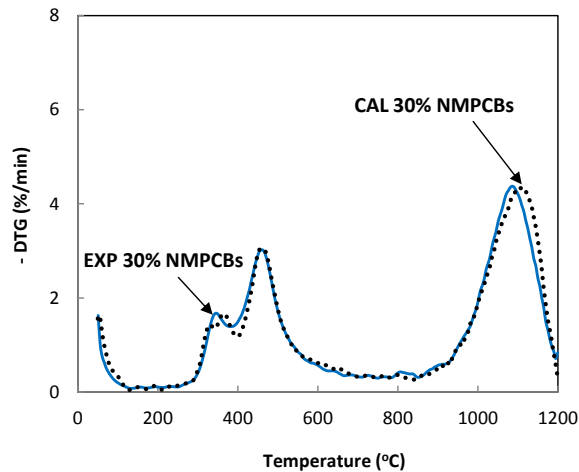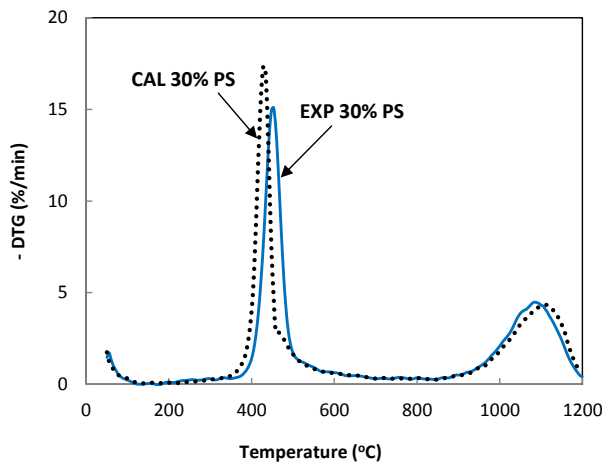
365

366   **Figure 3: Comparison of experimental and calculated DTG curves of (a) coal/oat straw, (b) coal/NMPCBs,**
367   **(c) coal/tyre and (d) coal/polystyrene blends.**

3.5   Mechanism of interactions

369   In spite of blending equal proportions of different carbonaceous materials with coal, intensity

370   and temperature at which interactions took place varied considerably. High level of volatile

371   content and high reactivity of carbonaceous materials were the reasons for the existence of

372   interactions in the blends [19, 37]. As previously explained, at both low and high blending

373   ratios, coal/polystyrene blends exhibited the highest interactions during devolatilisation stage.

374   This was due to the generation of large amount of reactive free radicals from polystyrene

375   cracking of as a result of containing a relatively higher amount of volatiles. The free radicals

376   were released through thermal decomposition of polystyrene, which react with coal and

377   enhance the devolatilisation and coal char gasification. In addition, the volatiles generated by

378   coal can react with the gases resulted from the cracking of the heavy volatiles as well as light

379   molecules (mostly hydrocarbon) derived from polystyrene. Therefore, a sluggish increment of

380   the secondary char generation is observed because of the inhibition of reverse Boudouard

381   reaction. Furthermore, the maximum weight loss rate also influences the generation of

382   different kinds of radicals. The rate of radicals formation is increased by their stability; hence

383   the conversion rate is greater when more stable radicals formed during devolatilisation

384   process [38]. Applying this concept to carbonaceous materials, the maximum weight loss rate

385   obtained by polystyrene is very high and this suggests the generation of stable radicals. This

386   phenomenon also assisted to the significant interactions during devolatilisation stage. On the

387   other side, even though NMPCBs had lower amount of volatiles, stronger interactions were

388   observed at devolatilisation stage. This behaviour was due to epoxy resin, a main part of

389   NMPCBs, which decomposed at relatively low temperature because of its high reactivity.

390 The interactions can also be caused by the catalytic effect of alkali and alkaline earth metals

391 (AAEM) contained in ash of the original samples [37, 39, 40]. It is reported that AAEM,

392 particularly, Ca and K species are active catalyst for gasification process [41, 42].

393 In the beginning of decomposition process, calcium, potassium and the other AAEM species

394 are combined with the carboxyl and phenolic groups, forming organic molecules in coal or

395 carbonaceous sample [43]. At the same time, the organic substances in the solid surface are

396 transformed to a micro-crystalline char, favouring the structure of char to become more

397 porous which enhances the reactivity in gasification [42].

398 Afterwards, this porous char adsorbs the AAEM onto its surface during the volatile-char

399 interactions stage [44]. Moreover, the presence of intermediate alkali-surface compounds

400 creates a bigger gap between AAEM and carbon which result in significant volume

401 expansion. These behaviours therefore contribute to the promotion of the gasification reaction

402 through weakening the carbon-carbon bonds present between layers [41].

403 As seen in Table 1, oat straw ash has demonstrated mostly the highest amount of these AAEM

404 among the others. In particular, CaO and K_2O in oat straw were found to be 10.6 wt% and

405 32.8 wt%, respectively, which were essential components for catalytic effect. Therefore, these

406 mainly contributed to the highest interactions in char gasification stage shown by coal/oat

407 straw blends compared with other blends. Meanwhile, the ash from NMPCBs, tyre and coal

408 samples contain a comparable percentage of AAEM, much lower than those of oat straw.

409 Moreover, ash compositional data showed that oat straw had high silica content which has

410 been demonstrated to reduce the reactivity of char [45]. However, the proportion of silica in

411 the other samples were relatively similar to each other, thus, the overall effect from silica was

412 assumed to be similar regardless of types of samples. Similarly, alumina also acts as a

413 deactivator for the catalytic effect [46]. As the lowest percentage of Al_2O_3 (2.2 wt%) was

414 observed in oat straw ash, so that oat straw had the least obstacle to undergo the catalytic

415 activities. It is worth noting that coal/tyre blend exhibited higher interactions than NMPCBs at

416 high blending ratio despite both had almost equal percentage of AAEM. The reason behind

417 these characteristics can be explained by Fe_2O_3 in the ash. Previous study revealed that metal

418 oxide such as Fe_2O_3 increased the gasification activity of coal due to the catalytic effect in

419 CO_2 gasification [47]. As tyre ash contain higher percentage of Fe_2O_3 (45.1 wt%), hence, it

420 could act as a catalyst for char-CO_2 reaction.

4 Conclusion

422 CO_2 co-gasification of coal with four different waste carbonaceous materials was investigated

423 in a thermogravimetric analyser. The influence of waste origin on the mechanism of

424 interactions was also discussed. The main findings are summarised as follows: (i) significant

425 high volatiles content of carbonaceous materials could plays a vital role in enhancing the

426 degree of interactions during devolatilisation stage; (ii) AAEM metals content such as CaO

427 and K_2O had a key influence on strong interactions in char gasification stage due to their

catalytic effect; (iii) the improvement of coal gasification performance is noticed as

demonstrated by its gasification characteristics such as initial decomposition temperature and

final mass loss temperature with the addition of carbonaceous materials, irrespective of stage

at which the interactions occurred. The best performances of gasification process in CO_2

atmosphere were achieved by using polystyrene and oat straw as carbonaceous materials to be

blended with coal. These phenomena were as expected mainly due to polystyrene having the

highest volatiles content whereas oat straw presented the catalytic effect from its AAEM

metals. Furthermore, the comparison between co-pyrolysis and CO_2 gasification processes by

using RMSII values confirmed the influence of CO_2 as a gasifying agent on the presence of

interactions in the blends. Hence, these experimental findings have confirmed that CO_2

gasification of coal can be considerably improved by adding polystyrene and oat straw into

the process.

Acknowledgement

5 References

1. Wu, T., et al., *Characteristics and synergistic effects of co-firing of coal and carbonaceous wastes.* Fuel, 2013. **104**(0): p. 194-200.

2. Sami, M., K. Annamalai, and M. Wooldridge, *Co-firing of coal and biomass fuel blends.* Progress in Energy and Combustion Science, 2001. **27**(2): p. 171-214.

3. Pan, Y.G., et al., *Fluidized-bed co-gasification of residual biomass/poor coal blends for fuel gas production.* Fuel, 2000. **79**(11): p. 1317-1326.

4. Seo, M.W., et al., *Gasification characteristics of coal/biomass blend in a dual circulating fluidized bed reactor.* Energy & Fuels, 2010. **24**(5): p. 3108-3118.

5. Wang, L., et al., *CO_2 Gasification of Chars Prepared from Wood and Forest Residue: A Kinetic Study.* Energy & Fuels, 2013. **27**(10): p. 6098-6107.

6. Skodras, G., G. Nenes, and N. Zafeiriou, *Low rank coal – CO_2 gasification: Experimental study, analysis of the kinetic parameters by Weibull distribution and compensation effect.* Applied Thermal Engineering, 2015. **74**(0): p. 111-118.

7. Lahijani, P., et al., *CO_2 gasification reactivity of biomass char: Catalytic influence of alkali, alkaline earth and transition metal salts.* Bioresource Technology, 2013. **144**(0): p. 288-295.

8. Butterman HC, C.M., *CO_2 as a Carbon Neutral Fuel Source via Enhanced Biomass Gasification.* Environ. Sci. Technol., 2009(43): p. 9030–9037.

9. Edreis, E.M.A., G. Luo, and H. Yao, *Investigations of the structure and thermal kinetic analysis of sugarcane bagasse char during non-isothermal CO_2 gasification.* Journal of Analytical and Applied Pyrolysis, 2014. **107**(0): p. 107-115.

10. Kirtania, K., et al., *Comparison of CO_2 and steam gasification reactivity of algal and woody biomass chars.* Fuel Processing Technology, 2014. **117**(0): p. 44-52.

11. Khalil, R., et al., *CO_2 gasification of biomass chars: a kinetic study.* Energy & Fuels, 2008. **23**(1): p. 94-100.

12. Sircar, I., et al., *Experimental and modeling study of pinewood char gasification with CO_2.* Fuel, 2014. **119**(0): p. 38-46.

13. Lewis, A.D., E.G. Fletcher, and T.H. Fletcher, *Pyrolysis and CO_2 Gasification Rates of Biomass at High Heating Rate Conditions.* 2013.

14. Huo, W., et al., *Study on CO_2 gasification reactivity and physical characteristics of biomass, petroleum coke and coal chars.* Bioresource Technology, 2014. **159**(0): p. 143-149.

15. Pohořelý, M., et al., *CO_2 as moderator for biomass gasification.* Fuel, 2014. **117, Part A**(0): p. 198-205.

484   16.   Hanaoka, T., S. Hiasa, and Y. Edashige, *Syngas production by CO2/O2 gasification of*
485   *aquatic biomass.* Fuel Processing Technology, 2013. **116**(0): p. 9-15.

486   17.   BS/EN15443:2011, *Solid recovered fuels. Methods for the preparation of the*
487   *laboratory sample.* 2011.

488   18.   ISO17246:2010, *Coal - Proximate analysis.* 2010.

489   19.   Edreis, E.M.A., et al., *Synergistic effects and kinetics thermal behaviour of petroleum*
490   *coke/biomass blends during H2O co-gasification.* Energy Conversion and
491   Management, 2014. **79**(0): p. 355-366.

492   20.   Gil, M.V., et al., *Thermal behaviour and kinetics of coal/biomass blends during co-*
493   *combustion.* Bioresource Technology, 2010. **101**(14): p. 5601-5608.

494   21.   Wang, Q., et al., *Interactions and kinetic analysis of oil shale semi-coke with cornstalk*
495   *during co-combustion.* Applied Energy, 2011. **88**(6): p. 2080-2087.

496   22.   Butterman, H.C. and M.J. Castaldi. *CO2 enhanced steam gasification of biomass*
497   *fuels.* in *16th Annual North American Waste-to-Energy Conference.* 2008. American
498   Society of Mechanical Engineers.

499   23.   Basu, P., *Combustion and gasification in fluidized beds.* 2006: CRC press.

500   24.   Sahu, S.G., N. Chakraborty, and P. Sarkar, *Coal–biomass co-combustion: An*
501   *overview.* Renewable and Sustainable Energy Reviews, 2014. **39**(0): p. 575-586.

502   25.   Xie, Z. and X. Ma, *The thermal behaviour of the co-combustion between paper sludge*
503   *and rice straw.* Bioresource Technology, 2013. **146**(0): p. 611-618.

504   26.   Basu, P., *Biomass gasification and pyrolysis: practical design and theory.* 2010:
505   Academic press.

506   27.   Backreedy, R.I., et al., *Modeling the reaction of oxygen with coal and biomass chars.*
507   Proceedings of the Combustion Institute, 2002. **29**(1): p. 415-421.

508   28.   Wang, X., et al., *Kinetics investigation on the combustion of biochar in O2/CO2*
509   *atmosphere.* Environmental Progress & Sustainable Energy, 2015. **34**(3): p. 923-932.

510   29.   Wu, W. and K. Qiu, *Vacuum co-pyrolysis of Chinese fir sawdust and waste printed*
511   *circuit boards. Part I: Influence of mass ratio of reactants.* Journal of Analytical and
512   Applied Pyrolysis, 2014. **105**(0): p. 252-261.

513   30.   Quan, C., A. Li, and N. Gao, *Thermogravimetric analysis and kinetic study on large*
514   *particles of printed circuit board wastes.* Waste Management, 2009. **29**(8): p. 2353-
515   2360.

516   31.   Martínez, J.D., et al., *Waste tyre pyrolysis – A review.* Renewable and Sustainable
517   Energy Reviews, 2013. **23**: p. 179-213.

518   32.   Chen, F. and J. Qian, *Studies of the thermal degradation of waste rubber.* Waste
519   Management, 2003. **23**(6): p. 463-467.

520   33.   Zhang, Y., et al., *Effect of fuel origin on synergy during co-gasification of biomass*
521   *and coal in CO2.* Bioresource Technology, 2016. **200**: p. 789-794.

522 34. Chen, T., et al., *Key thermal events during pyrolysis and CO2-gasification of selected*
523 *combustible solid wastes in a thermogravimetric analyser.* Fuel, 2014. **137**: p. 77-84.
524 35. Lai, Z., et al., *Thermogravimetric analysis of the thermal decomposition of MSW in*
525 *N2, CO2 and CO2/N2 atmospheres.* Fuel Processing Technology, 2012. **102**: p. 18-23.
526 36. Grammelis, P., et al., *Pyrolysis kinetics and combustion characteristics of waste*
527 *recovered fuels.* Fuel, 2009. **88**(1): p. 195-205.
528 37. Tchapda, A.H. and S.V. Pisupati, *A review of thermal co-conversion of coal and*
529 *biomass/waste.* Energies, 2014. **7**(3): p. 1098-1148.
530 38. Kiran, N., E. Ekinci, and C. Snape, *Recyling of plastic wastes via pyrolysis.*
531 Resources, Conservation and Recycling, 2000. **29**(4): p. 273-283.
532 39. Edreis, E.M.A., et al., *CO2 co-gasification of lower sulphur petroleum coke and sugar*
533 *cane bagasse via TG–FTIR analysis technique.* Bioresource Technology, 2013.
534 **136**(0): p. 595-603.
535 40. Nemanova, V., et al., *Co-gasification of petroleum coke and biomass.* Fuel, 2014. **117,**
536 **Part A**(0): p. 870-875.
537 41. Huang, Y., et al., *Effects of metal catalysts on CO2 gasification reactivity of biomass*
538 *char.* Biotechnology Advances, 2009. **27**(5): p. 568-572.
539 42. Mitsuoka, K., et al., *Gasification of woody biomass char with CO2: The catalytic*
540 *effects of K and Ca species on char gasification reactivity.* Fuel Processing
541 Technology, 2011. **92**(1): p. 26-31.
542 43. Quyn, D.M., et al., *Volatilisation and catalytic effects of alkali and alkaline earth*
543 *metallic species during the pyrolysis and gasification of Victorian brown coal. Part*

544 *IV. Catalytic effects of NaCl and ion-exchangeable Na in coal on char reactivity☆.*

545 Fuel, 2003. **82**(5): p. 587-593.
546 44. Li, X. and C.-Z. Li, *Volatilisation and catalytic effects of alkali and alkaline earth*
547 *metallic species during the pyrolysis and gasification of Victorian brown coal. Part*
548 *VIII. Catalysis and changes in char structure during gasification in steam.* Fuel, 2006.
549 **85**(10–11): p. 1518-1525.
550 45. Kannan, M.P. and G.N. Richards, *Gasification of biomass chars in carbon dioxide:*
551 *dependence of gasification rate on the indigenous metal content.* Fuel, 1990. **69**(6): p.
552 747-753.
553 46. Kajita, M., et al., *Catalytic and Noncatalytic Mechanisms in Steam Gasification of*
554 *Char from the Pyrolysis of Biomass†.* Energy & Fuels, 2009. **24**(1): p. 108-116.
555 47. He, P., et al., *Simultaneous Low-Cost Carbon Sources and CO2 Valorizations through*
556 *Catalytic Gasification.* Energy & Fuels, 2015. **29**(11): p. 7497-7507.
557
558